Transactions of the Materials Research Society of Japan 32[3] 615-618 (2007)

Numerical calculation of Joule heat generated by susceptor heating with induction for waste vitrification

J. S. Park, H. Shimada*, S. Taniguchi, K. Betsumori**, H. Morino**and S. Yamada**
Graduate School of Environmental Studies, Tohoku University, Sendai, Miyagi 980-8579
Fax: 81-22-795-7302, e-mail: jong-soo-park@mail.tains.tohoku.ac.jp
* Department of Metallurgy, School of Engineering, Tohoku University, Sendai, Miyagi 980-8579
Fax: 81-22-795-7302, e-mail: a3tb4053@stu.material.tohoku.ac.jp
**Engineering Environmental Technology Development Center, Hokuriku Electric Power Company, Toyama 930-0848
Fax: 81-76-441-5297, e-mail: betsumori.keiichi@rikuden.co.jp

Morphological effect of a susceptor on Joule heat by induction heating was investigated. Numerical computation of Joule heat was based on mutual inductance model suggested by Tarapore and Evans. The calculated results were compared with experimental results. In experiment, susceptors were made of stainless steel or graphite with two shapes: cylinder-type (Φ40, or 50 mm $\times$ 80 mm) and tube-type (Φ50 $\times$ 80 mm). These were put on the center of a coil and then, their Joule heats were experimentally measured by a specific apparatus using water flow rate and temperature difference. Magnetic field is canceled out by eddy current in cylindrical stainless steel, whereas penetrated to the inside of tubular stainless steel. The calculated values corresponded well to the observed values, within error range of less than 5%. When maximum current of 1A was imposed into the coil, the cylindrical susceptor (Φ40 mm $\times$ 80 mm, stainless steel) placed at middle of the coil generated Joule heat of 9.1 $\times$ 10^{-3} W/A^2, higher than that of 5.4 $\times$ 10^{-3} at both ends of the coil. The graphite also showed the same tendency as stainless steel. With a decrease in thickness of the tubular susceptor, heat generation increased because inductive reactance effect deceased and current density became much higher. The tubular stainless steel (Φ50 mm $\times$ 80 mm, t / δ = 0.1) had extremely high heat generation (5.3 $\times$ 10^{-2} W/A^2), matching up to the experimental results. As a result, tubular susceptor heating may compensate various industrial melting systems for large energy consumption, as well as induction furnace.

Key words: tubular susceptor heating, Joule heat, numerical analysis, mutual inductance, inductive reactance

1. INTRODUCTION

Conventional furnaces are typically thought a machine that uses a heat source such as gas or electrical elements, which radiate energy to the partial surface of materials to be heated. Heat then conducts through the material based upon its surface temperature and thermal conductivity. This restricts the rate raised in temperature and the final temperature that the materials can be heated.

With these limitations in mind, induction heating has be proven to be a valuable tool that provides rapid, reliable heat for industrial applications to bonding, changing, or melting of materials. An induction furnace is actually an energy-transfer equipment rather than just a furnace. In this equipment, energy is transferred directly from an induction coil into the material through the electromagnetic field generated by alternating current. Since there is no external heat source and heat is generated within the material, the maximum temperature in induction furnace can be practically unlimited. However, modern progress has made an induction furnace in remarkably simple, cost-expansive heating method even though the essential principles of induction are well recognized. Especially, the method has extremely low efficiency in melting plastics and other non-conductive materials. In this case, induction furnace must incorporate susceptor heating. Employing a conductive susceptor can heat very effectively because it is used to capture the electromagnetic current. Graphite is often used for susceptor because it has good properties for induction: high resistivity, melting point and mechanical strength. Susceptor can also be made out of stainless steel, aluminum, silicon carbide, molybdenum, niobium and other conductors. The susceptor can be produced in the form of a crucible, tube, disk and so on, for example, crucible melting of radioactive waste [1], pipe bending by induction heating [2], CVD process in semiconductor manufacturing [3], etc.

In waste treatment, induction furnace has been also introduced as a melting furnace and developed a more-

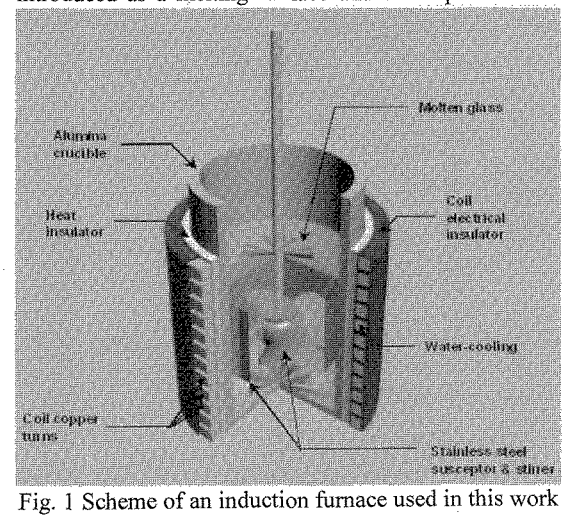

Fig. 1 Scheme of an induction furnace used in this work

advanced furnace, which roughly includes two types [4]: a hot-crucible furnace with susceptor (external heating) and a cold-crucible furnace without susceptor (internal heating). However, the hot-crucible furnace generates secondly waste from short life of the melting chamber and limits the maximum temperature due to heat source closed by water-cooling coil. The cold-crucible furnace, of course, has high energy loss when high frequency for directly induction heating is made.

This paper proposes a new induction furnace for high-energy efficiency, which combines internal heating with external heating, as shown in Fig. 1. For this proposal, Joule heat of susceptor with the shape, the size, and the position in the coil was investigated. Solutions of electromagnetic field were found by mutual inductance model suggested by Tarapore and Evans [5], and Joule heat was obtained from these results. The Joule heats calculated by the model were reliable in comparison with Joule heats measured by experiments.

2. THEORETICAL APPROACH

The solution of the electromagnetic field equations can be derived from the Maxwell equations. Maxwell equations represent one of the most clear and simple ways to state the fundamentals of electricity and magnetism. From them, one can develop most of the working relationships in the field. The equations are

$$\nabla \times \mathrm{E} = -\mu \frac{\partial \mathrm{H}}{\partial \mathrm{t}} \tag{1}$$

$$\nabla \times \mathrm{H} = \mathrm{J} \tag{2}$$

$$\nabla \cdot \mathrm{H} = 0 \tag{3}$$

where E, H and J are electric field, magnetic field and current density, respectively. μ is permeability. Ohm's law is necessary to solve the equations in addition to Maxwell equation.

$$\mathrm{J} = \sigma(\mathrm{E} + \mu \mathrm{V} \times \mathrm{H}) \tag{4}$$

where σ is electric conductivity and V is velocity. Now consider the application of these equations to the axisymmetric melt and coil arrangement depicted in Fig. 1. In Eq. (4), the second term may be neglected to a good approximation. Furthermore, we may regard them as 'phases':

$$\mathrm{E} = \mathrm{E}_0 e^{j\omega t} \tag{5}$$

$$\mathrm{H} = \mathrm{H}_0 e^{j\omega t} \tag{6}$$

$$\mathrm{J} = \mathrm{J}_0 e^{j\omega t} \tag{7}$$

Eq. (1) becomes

$$\nabla \times \mathrm{E} = -j\omega\mu \mathrm{H} \tag{8}$$

The vector potential A defined by

$$\mathrm{H} = \frac{1}{\mu} \nabla \times \mathrm{A} \tag{9}$$

$$\nabla \cdot \mathbf{A} = \mathbf{0} \tag{10}$$

With these definitions, Eq. (2) can be simplified and integrated over a finite volume that includes both the material and the coils.

$$\mathrm{A} = \frac{\mu}{4\pi} \int_{\mathrm{vol}} \frac{\mathrm{J}'}{|\mathrm{r}'|} dV' \tag{11}$$

where |r'| is the distance from the current to the point, where the potential is evaluated, and J' presents that currents within material and coil cause inducted current at the point. According to Eq. (8) and Eq. (9)

$$\nabla \times \mathrm{E} = \nabla \times (-j\omega \mathrm{A}) \tag{12}$$

Finally, we obtain

$$\mathrm{J}_{\mathrm{material}} = -\frac{j\omega\sigma\mu}{4\pi} \int_{\mathrm{vol}} \frac{\mathrm{J}'}{|\mathrm{r}'|} dV' \tag{13}$$

For a cylindrical induction furnace, Eq. (13) becomes

$$\mathrm{J}_\theta(r,z) = -j\omega\sigma\mu \int_0^H \int_0^R \mathrm{J}_\theta(r',z') f(r,r',z,z') dr' dz' - j\omega\sigma\mu \sum_{coil} I_{\theta coil}(r_{coil}, z_{coil}) \times f(r, r_{coil}, z, z_{coil}) \tag{14}$$

where H and R are height and radius of material in solenoid, respectively. In addition, Joule heat, W_Θ (r, z), is

$$\mathrm{W}_\theta(r,z) = \frac{|\mathrm{J}_\theta(r,z)|^2}{2\sigma} \tag{15}$$

and total Joule heat, W (J/s), can be evaluated by integration on the total volume, as following:

$$\mathrm{W\,(J/s)} = \int_0^H \int_0^R \frac{|\mathrm{J}_\theta(r,z)|^2}{2\sigma} 2\pi r dr dz \tag{16}$$

3. EXPERIMENTAL

The induction-melting furnace (20kW, 30kHz) was coupled with a susceptor installed at the center in the furnace, as shown in Fig. 1. This gave an advantage to minimize heat losses taken away to the water-cooling coil. A solenoid coil of the furnace consisted of 12-turns (Φ10 mm copper tube), diameter of 110 mm and height of 120 mm.

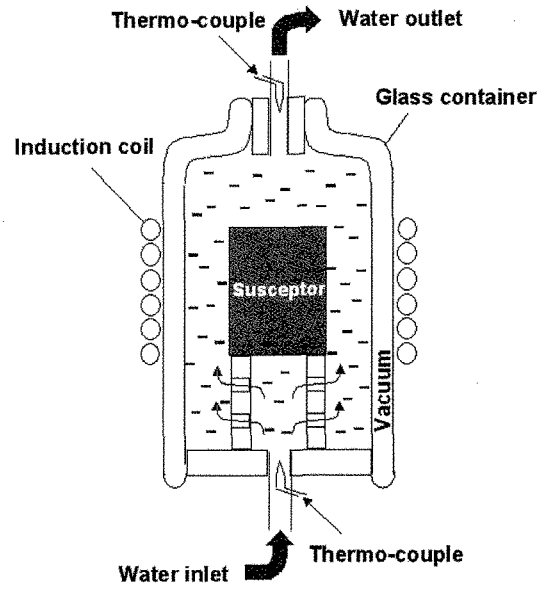

Fig. 2 Scheme of experimental apparatus measuring Joule heat

Fig.2 shows schematic diagram of experimental apparatus that was used to measure Joule heats generated in the susceptor fixed in a glass bottle. The bottle (Φ90 mm × H400 mm) made of two concentric transparent borosilicate glasses tubes (Pyrex), in which the double wall vacuum was to prevent Joule heat from heat losses. The apparatus measured water flow rate through the tube and temperature difference at both ends and then, the heat generations of susceptors, W_e (J/s), were calculated by the following equation:

$$W_e\,(\mathrm{J/s}) = \rho c_P V (T_{out} - T_{in}) \qquad (17)$$

where ρ is the density, V is the volumetric flow rate, and c_p is the specific heat of water. Taniguchi et al. have even proved the accuracy of the mutual inductance model in range of $f = 3.0 \times 10^4 \sim 2.0 \times 10^5$ Hz [6]

4. RESULTS AND DISCUSSION

Fig. 3 shows magnetic field and Joule heat distributions with a susceptor placed into the furnace, in change of frequency. The field trying to pass through the susceptor is canceled out by opposite field generated by eddy currents within it. This phenomenon becomes stronger as the frequency increased.

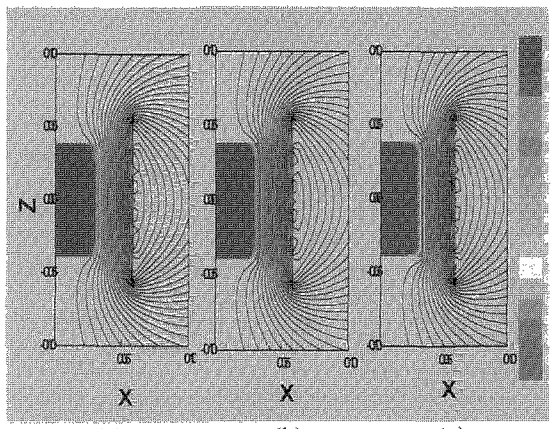

(a) (b) (c)

Fig. 3 Magnetic field and Joule heat with a susceptor inside of the furnace: f = (a) 10 kHz, (b) 30 kHz and (c) 100 kHz

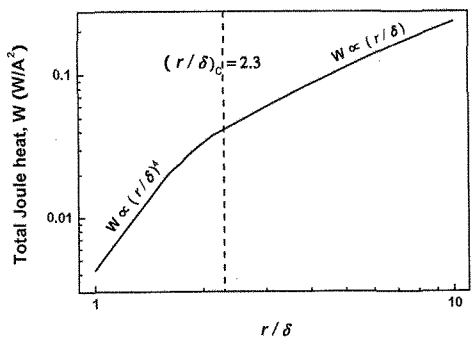

Fig. 4 Changes in Joule heat generation with r/δ (r = 50 mm (constant), f controlled)

Total Joule heats were calculated with a change in a frequency through the proposed model at a fixed coil current, 1A (max.) and were plotted with r/δ (radius/skin depth), as shown in Fig. 4. In general, Joule heat is proportional to the square of the frequency under critical frequency, f_C. On the other hand, this is linear with (r/δ) above f_C [7]. Fig. 4 shows that $(r/\delta)_C$ is approximately 2.3, which proves that the numerical results conform to the laws of electromagnetism.

The field gradients cause the difference of the heat generation, depending on position of the susceptor in the coil [8]. To clarify furthermore the characteristics of the model, the results of numerical computation were compared with experimental results (Fig. 5). The susceptor (Φ40 mm × 80 mm) generated Joule heat in the range of 5.2 ~ 9.1 × 10^{-3} W/A^2 and the field was concentrated on the center of the cylindrical coil. The mutual inductance model eventually gave an acceptable accuracy between calculations and experiments, in error by less than ± 5 %.

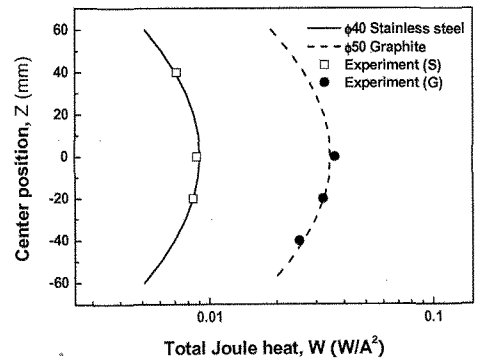

Fig 5 Total heat generation as vertical position of the cylindrical susceptor changed in the furnace

Effect of susceptor shape on Joule heat was further evaluated with a conversion of cylinder to tube. In stainless-steel susceptor (Φ50 mm × 80 mm), maximum Joule heat was generated at t/δ (tube thickness/skin depth) of 0.1, which was less then skin depth, and approximately 3.6 times higher than that of cylinder-type (Fig. 6). We define it as critical thickness, $(t/\delta)_C$. Critical thickness became thinner with an increase in frequency (f) and a radius of susceptor (r). The results from the experiments corresponded well to the results from the numerical computation, as shown in fig. 6.

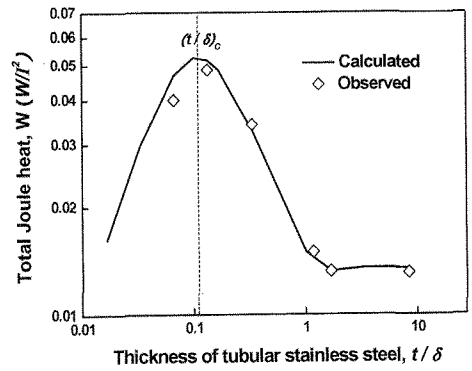

Fig 6 Total heat generation of tubular susceptor (Φ50 mm × 80 mm stainless steel) as its wall changed

Fig. 7 shows total induced currents and mean current densities on cross section of tube wall with a change of the thickness. As the thickness decreases, the total induced currents also decrease, but the mean current densities show countertrend. Moreover, total induced currents and mean current densities have slope change at same position as critical thickness. Compared with Fig. 6, Joule heat increases over critical thickness because induced currents are concentrated on smaller cross section. On the other hand, under critical thickness, it decreases by the rapid reduction of total induced current.

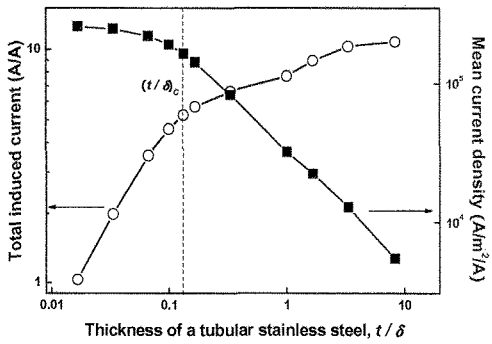

Fig 7 (a) Total induced current and (b) mean current density with thickness of tube wall (Φ50 mm × 80 mm)

This trend of Joule heat should be relative to inductive reactance: critical thickness can be thought of as a changing point of susceptor sensitivity to the magnetic field by changing dimensions. Detail analogical analysis will be discussed on other paper and, here, fundamental knowledge is mentioned.

Without respect to inductive reactance, Joule heat for tubular susceptor in cylindrical coil is

$$W(\mathrm{W}) = \frac{8\pi^5 f^2 \mu_r^{\,2} n^2 I^2 h}{\rho}(r_{out}^{\,4} - r_{in}^{\,4}) \times 10^{-14} \quad (18)$$

where μ_r, n, I and h are relative permeability of the susceptor, number of turns in the coil, directly imposed current and height of the susceptor, respectively [9]. This means that total Joule heat reduced with a decrease in thickness of a tube. However, the inductive reactance should be ignored no longer if the number of turns and frequency is increased, as follows:

$$X_L = 2\pi f L \quad (19)$$

where X_L and L are inductive reactance and inductance. Assuming that a susceptor is composed of small coil. The cylindrical susceptor looks as if an assembly closely fills with the coils. When induced currents are flowing through the coils, the current should cause the reduction of current flow in other coil. This is because the magnetic field from one coil interacts with that from other coils. From this point of view, the tubular susceptor could minimize the effect of inductive reactance on susceptor heating. Then, it could maximize Joule heat, more than 3.6 times, at critical thickness.

5. CONCLUSIONS

In susceptor heating with induction, the characteristics of Joule heat generation was investigated. The numerical values computed by mutual inductance model complied well with the laws of general electromagnetism. Moreover, it showed high accuracy in range of ±5%, compared with the experimental values. Joule heat with the position of susceptor in the coil has similar patterns, independent of materials. The cylindrical susceptor (Φ 40 mm × 80 mm) at center has higher heat generation of ~1.8 times compared with that at both ends. Conversion of cylinder-type to tube-type in susceptor shape gave the effect to the elimination of inductive reactance. As a result, a large amount of heat was generated because eddy currents concentrated on the smaller cross section of susceptor, even though total current reduced. The heat from tubular susceptor of stainless-steel (Φ50 mm × 80 mm, t = 0.3 mm) was approximately 3.6 times higher than that of $t > \delta$. Consequently, the tubular susceptor heating would be applied to various induction melting system as well as waste vitrification in energy efficient aspect, for example, elimination of inductive reactance, reduction of heat loss to water-cooling coil and homogeneity of heat distribution.

ACKNOWLEDGEMENT

This work was particularly supported by Hokuriku Electric Power Company for the project of asbestos deposal, which was established by New Energy and Industrial Technology Development Organization (NEDO) in Japan, (*NEDO- 06001439-0*). In addition, this work was partially supported by Korea Research Foundation Grant funded by Korea government (MOEHRD, Basic Research Promotion Fund) (*KRF-2005-215-D00177*).

REFERENCES

[1] K. Raj, *J. Nucl. Energ. Sci. Tech.*, 1, 148-63, 2005
[2] N. A. Sypchenko, *Chem. Petrol. Eng.*, 2, 614, 1966
[3] D. R. Biswas, *J. Mater. Sci.*, 21, 2217-23, 1986
[4] K. Guilbeau, A Giordana, W. G. Ramsey, N. Shulyak, A. Aloy and R. A. Soshnikow, *Am. Ceram. Soc. Bull.*, 83, 38-40, 2004
[5] E. D. Tarapore, J. W. Evans, *Metall. T. B*, 7B, 343-51, 1976
[6] S. Taniguchi, A. Kikuchi, *Tetsu to Hagane.*, 78, 753-60, 1992
[7] S. Taniguchi, A. Kikuchi, *Tetsu to Hagane.*, 70, 846-58, 1984
[8] J. G. Lee, "Practical high-frequency induction heating", Jinyoungsa (1996) pp. 293-4
[9] K. Takahasi, Y. Kubota, h. Kaneda et al, "Fundamentals and application of high frequency", Tokyo (1990) pp. 2-10

(Received January 20, 2007;Accepted May 10, 2007)